



<b>Title</b>	Detection of charge dynamics of a tetraphenylporphyrin particle using GaAs-based nanowire enhanced by particle-metal tip capacitive coupling
<b>Author(s)</b>	Okamoto, Shoma; Sato, Masaki; Sasaki, Kentaro; Kasai, Seiya
<b>Citation</b>	Japanese Journal of Applied Physics (JJAP), 56(6), 06GK02 <a href="https://doi.org/10.7567/JJAP.56.06GK02">https://doi.org/10.7567/JJAP.56.06GK02</a>
<b>Issue Date</b>	2017-06
<b>Doc URL</b>	<a href="http://hdl.handle.net/2115/70628">http://hdl.handle.net/2115/70628</a>
<b>Rights</b>	© 2017 The Japan Society of Applied Physics
<b>Type</b>	article (author version)
<b>File Information</b>	JJAP2017_56_MN16086.pdf



[Instructions for use](#)

# **Detection of charge dynamics of a tetraphenylporphyrin particle using GaAs-based nanowire enhanced by particle-metal tip capacitive coupling**

Shoma Okamoto, Masaki Sato, Kentaro Sasaki, and Seiya Kasai\*

*Research Center for Integrated Quantum Electronics and Graduate School of Information Science & Technology, Hokkaido University, Sapporo 060-8628, Japan*

\*E-mail: kasai@rciqe.hokudai.ac.jp

We investigate a detection technique of charge dynamics of a molecular particle using a GaAs-based nanowire where the charge sensitivity is locally enhanced by particle-metal tip capacitive coupling. By equivalent circuit analysis, it was clarified that the nanowire channel potential becomes sensitive to the molecular particle on the nanowire when the particle is capacitively coupled with a metal tip. The concept was demonstrated using a GaAs-based nanowire with tetraphenylporphyrin (TPP) particles on its surface and a measurement system integrating an atomic force microscope (AFM) and a dynamic current measurement monitor/spectrum analyzer. When the metal tip was in contact with a TPP particle on the nanowire under an appropriate tip bias condition, random telegraph signal (RTS) noise was imposed on the nanowire current, suggesting the increase in sensitivity to the charge state of the particle by the metal tip contact. We discussed the origin of the RTS noise through analysis of the time constant of RTS noise, RTS amplitude, and noise spectrum.

## 1. Introduction

Extensive research studies have been made on single-molecule electronics aiming at information processing on the basis of the control of the charge dynamics in single-molecule networks<sup>1-6)</sup>. In the primary stage of the investigation of such system, the detection of dynamic charge behavior of the single molecule is indispensable. Thus far, scanning probe techniques achieving atomic-scale spatial resolution have been used for characterizing the molecules<sup>7-11)</sup>. However, their time resolution is often of millisecond order<sup>10,11)</sup>, because of the high impedance in the tip and the molecule. For the real-time detection of the charge state in individual molecules, it is necessary to develop a high-speed small-charge detection technique. In this paper, we investigate a detection technique of the dynamic charge state of molecules combining two techniques: dynamic molecule charge detection using a GaAs-based nanowire field-effect transistor (FET) having a metal gate<sup>12)</sup> and a GaAs surface trap detection technique based on the capacitive coupling between a conductive atomic force microscope (AFM) tip and a surface trap<sup>13)</sup>. In the former technique, the charge of the molecules in the metal gate periphery is selectively reflected in a GaAs nanowire current owing to the metal gate-molecule capacitive coupling. The semiconductor-based nanowire has a good potential for a high-speed charge detector, because of high sensitivity to surface charge<sup>14-18)</sup>. In particular, the GaAs-based nanowire possesses a high-speed response capability owing to the high electron mobility<sup>19)</sup>. This also achieves low background noise compared with Si MOSFETs<sup>20,21)</sup>. In the latter technique, we access the discrete surface trap using an AFM system, and the charge state of the trap is detected in terms of current noise. We found that this system has a single electron charge detection capability<sup>13)</sup>. In the detection technique investigated here, the metal gate of the GaAs-based nanowire FET is replaced by

a metal AFM tip to access the aimed molecule. The feasibility of the field effect by the conductive AFM tip was already demonstrated in the detection of the static spatial distribution of carriers in quantum devices<sup>22-24</sup>). In this paper, a preliminary demonstration of our concept is made by using a tetraphenylporphyrin (TPP) particle dispersed on the GaAs nanowire.

## 2. Concept

The basic concept of the detection of the dynamic charge state of molecules is shown in Fig. 1. The molecules are dispersed on a GaAs nanowire surface as shown in Fig. 1(a). A GaAs nanowire having two-dimensional electron gas (2DEG) is used as a small charge detector, which has high surface charge sensitivity and achieves a high-speed response owing to the high electron mobility of the 2DEG channel<sup>13</sup>). A target molecule is selectively detected by making a capacitive coupling with a metal tip. The metal tip works as a tiny metal gate for the nanowire or the molecule. Figure 1(b) shows the cross-sectional structure of the nanowire together with its equivalent circuit; a molecule is capacitively coupled with the metal tip,  $C_1$ . With the analysis of the equivalent circuit in Fig. 1(b), variation of the channel potential by the charging and discharging of a discrete charge  $e$  in the molecule,  $\Delta V$ , is obtained as

$$\Delta V = \frac{C_1 e}{C_1 C_2 + C_2 C_3 + C_3 C_1}, \quad (1)$$

where  $C_2$  is the tunnel capacitance between the molecule and the GaAs channel.  $C_3$  is the capacitance between the GaAs channel and the ground. It is found that, when the molecule is capacitively coupled with the metal, that is,  $C_1 > 0$ , the exchange of the charge  $e$  between the molecule and the channel is reflected in the channel potential and then the nanowire current is modulated. Then, random charging and discharging of the molecule in contact with

the metal is expected to cause random transitions between two states of the nanowire current, referred to as random telegraph signal (RTS) noise. Analysis of the charging and discharging time constants will provide us information of the molecule energy state. Previously, we demonstrated this detection mechanism using a Schottky gate GaAs nanowire FET in which the metal gate couples with several molecules in the gate periphery<sup>12)</sup>. In order to access an aimed molecule, we replace the metal gate with a conductive AFM tip.

### 3. Experimental procedure

Figure 1(a) shows the experimental setup for demonstrating our concept. A GaAs-based nanowire device with molecules dispersed on the surface was placed in a tip-bias type AFM system (JPK instruments, Nanowizard). The metal tip was a commercially available platinum-iridium (PtIr)-coated Si cantilever. In this study, to confirm the basic concept, a TPP particle was used as measured substance instead of a single molecule. A light-emitting diode (LED) of 403 nm wavelength was placed above the sample for exciting an electron in TPP. The wavelength overlapped the TPP absorption band<sup>25)</sup>. The LED power was 0.1 mW. The drain current and noise spectrum in the nanowire were measured using a conventional semiconductor parameter analyzer and a real-time spectrum analyzer together with a low-noise current amplifier (LNA), respectively. The time resolution was 41  $\mu$ s. In this measurement system, the current could be measured while maintaining the AFM tip contact with the nanowire or the TPP particle. To avoid the unintentional excitation of the charge in the particle and the nanowire, the laser for detecting the AFM cantilever displacement was turned off in the current measurement. The drift of the stage was sufficiently small for sampling the nanowire current. All the measurements were carried out at room temperature

(RT) in air ambient.

The GaAs-based nanowire was fabricated on an AlGaAs/GaAs heterostructure having the 2DEG by electron beam lithography and wet chemical etching. The heterostructure consisted of a 60 nm AlGaAs top barrier, a Si delta-doped layer, a 20 nm undoped GaAs channel, a 10 nm AlGaAs bottom barrier, and an undoped GaAs buffer on a semi-insulating (001) GaAs substrate. The 2DEG electron mobility  $\mu$  was  $7,100 \text{ cm}^2\text{V}^{-1}\text{s}^{-1}$  and the sheet density  $n_s$  was  $7.8 \times 10^{11} \text{ cm}^{-2}$  at RT. The length  $L$  and the width  $W$  of the fabricated nanowire were  $4 \text{ }\mu\text{m}$  and  $200 \text{ nm}$ , respectively. Ni/Ge/Au/Ni/Au ohmic contacts were formed for the source and drain electrodes.

A uniform surface dispersion of a small amount of TPP was important for our experiment. We applied the electrostatic deposition method <sup>26)</sup> for TPP dispersion. In this method, the machine sprayed the mists containing the molecules, which were charged by a high electric field. We used a commercial deposition system (Nagase Techno-engineering Micro Mist Coater). The distance between the sample and the nozzle was  $5 \text{ cm}$  and the applied voltage was  $14 \text{ kV}$ . Note that the solution should have a permittivity higher than  $15\epsilon_0$  ( $\epsilon_0$ : vacuum permittivity) for the electrostatic deposition, whereas the solvent should have a permittivity lower than  $7.6\epsilon_0$  for the dissolution of TPP. We found that the mixed solution with 70% acetone and 30% xylene could achieve both TPP dissolution and the electrostatic deposition.

## **4. Experimental results**

### *4.1 Electrostatic effect of a metal AFM tip on nanowire current*

First, we examined the electrostatic effect of the vertical tip position. In this study, the change in the vertical tip position,  $\Delta Z$ , was defined as the distance from the object surface;  $\Delta Z$  was

zero when the tip was in contact with the object surface. The camber of the cantilever was 13 nm and the calibrated value considering the camber was used for measuring the vertical tip position. Figure 2(a) shows an AFM image of the fabricated nanowire. The electrostatic effect was characterized when the AFM tip position was in the center of the nanowire. Figure 2(b) shows the vertical tip position dependence of the drain current  $I_{DS}$ . Here, the tip bias  $V_{tip}$  was 0 V and the drain voltage  $V_{DS}$  was 0.5 V. The current was decreased as the metal tip approached the nanowire. This indicated that the surface potential of the nanowire was increased by a large work function of the PtIr tip, approximately 5.6 eV<sup>27</sup>). Figure 2(c) plots the current and root mean square (RMS) of the drain current noise as a function of  $\Delta Z$ . The electrostatic effect of the tip was nonlinearly increased as the tip approached the nanowire. On the other hand, the drain current noise was approximately 10 nA, independent of the vertical tip position. Figure 2(d) plots the tip bias dependence of the measured current and RMS of the current noise. The vertical tip position was fixed at 20 nm from the nanowire surface. The current was systematically controlled by the tip bias and we obtained the mutual conductance between the tip and the nanowire,  $g_m$ , of 15.5 nS from the slope of the data. The drain current RMS was also 10 nA regardless of the tip bias. Thus, the noise was not affected by the vertical tip positioned and the tip bias. It was found that the metal tip worked as a very small metal gate that could electrostatically couple with the nanowire channel potential without affecting the current noise.

#### 4.2 Current and noise in nanowire with TPP particle

Then, we characterized the drain current after TPP dispersion on the nanowire surface. The AFM image of the sample after TPP dispersion is shown in Fig. 3(a) together with the tip positions. A few small TPP particles were observed on the nanowire. We confirmed that the

observed TPP particles maintained the basic property of the TPP molecule from the absorption spectrum in a macroscopic area by UV-visible spectroscopy and the micrometer-scale spatial distribution by 405 nm laser optical microscopy observation. The vertical position of the tip when the tip was in contact with the TPP particle, as indicated in Fig. 3(a), was 20 nm from the nanowire surface. This height of the particle corresponded to the stack of twenty TPP molecules, which was estimated from the  $\pi$ - $\pi$  intermolecular distance<sup>28)</sup> and the thickness of the TPP molecule<sup>29)</sup>, assuming that planar-shaped TPP molecules were stacked on the nanowire in parallel to the surface plane<sup>30)</sup>.

Figures 3(b) and 3(c) show the drain currents where the tip was positioned on the GaAs nanowire surface and the TPP particle, respectively. The tip biases were 0 and 3 V. When the tip was positioned on the GaAs nanowire surface with  $\Delta Z = 20$  nm, the effect of the tip bias on the current was very small. On the other hand, when the tip was positioned on the TPP particle, the current was markedly increased by increasing the tip bias, even with  $\Delta Z = 20$  nm (the tip was 20 nm away from the TPP surface). This suggested that the Fermi level pinning of the GaAs surface was reduced by dispersing TPP molecules on the GaAs. We obtained a similar result in a Schottky gate nanowire FET, where TPP in the gate periphery enhanced the metal work function dependence of the nanowire surface potential<sup>12)</sup>. Further study is necessary to clarify the mechanism of the observed behavior. Note that the RTS noise appeared when the tip was positioned on the TPP particle at  $V_{\text{tip}} = +3$  V, as shown in Fig. 3(c). This indicated that the random charging and discharging of the discrete charge took place and the charge interaction between the molecule and the nanowire was enhanced by the metal tip and biasing. The transient time between the high and low states of the RTS noise was a few milliseconds, which could be detected using the measurement system having time resolution of 41  $\mu$ s.

Figures 3(d) and 3(e) show the drain currents measured under the light condition, without and with TPP particles, respectively. The incident photon flux for the 403 nm LED light with 0.1 mW was estimated to be 1.9 photons/s for a TPP molecule area. The current was increased by the light irradiation, because TPP worked as a photoexcited donor<sup>12)</sup>. On the other hand, the RTS noise at  $V_{\text{tip}} = +3$  V was unchanged even under light irradiation. This contradicted a previous study using the Schottky-gate nanowire FET with TPP particles, where the current noise markedly increased when the light was irradiated<sup>12)</sup>.

Figure 4 summarizes the low-frequency current noise spectra in the nanowire with TPP particles. We separately confirmed that, when there was no capacitive coupling between the metal and the TPP particle,  $1/f$  noise was dominant (not shown in the figure), which was the general noise spectrum in semiconductor FETs<sup>31,32)</sup>, including the GaAs nanowire devices<sup>20,21)</sup>. The gentle slope in the high-frequency region was brought by the noise floor of the measurement system. In addition, without the tip-TPP capacitive coupling, the noise spectra were hardly affected by the light irradiation, similar to a previous study using a Schottky gate GaAs nanowire FET<sup>12)</sup>. As shown in Fig. 4(a),  $1/f$  noise was also dominant even when the tip was in contact with the TPP particle at  $V_{\text{tip}} = 0$  V. On the other hand,  $1/f^2$  noise was imposed on the spectrum at  $V_{\text{tip}} = +3$  V as shown in Fig. 4(b). It is known that the RTS noise exhibits a Lorentzian spectrum having a  $1/f^2$  slope<sup>32,33)</sup>. The obtained spectra did not show a corner of the Lorentzian spectrum. This was simply because the corner frequency was lower than 10 Hz, less than the lower frequency limit of the measurement system. The characteristic frequencies from the time constants of the RTS noises in Figs. 3(c) and 3(e) were 3.2 Hz under the dark condition and 1.6 Hz under the light condition, respectively, which did not conflict with the observed spectra. The light irradiation did not have a significant effect on the noise power and the spectrum as shown in Figs. 4(c) and 4(d), in

agreement with the behavior of the currents shown in Fig. 3(e). There was no effect of the light on the current noise probably because the photon supply was too small to excite the molecule dealing with the observed RTS noise. Considering that 20 TPP molecules were stacked under the tip and a molecule in contact with the nanowire could be attributed to the current noise, the estimated photon supply to the bottom molecule was less than 0.1 photons/s. This small number of photons could not excite the molecule in the measured time range of 4 s. To see the effect of the light irradiation on the RTS noise, further high power light was necessary.

## 5. Discussion

First, let us consider that the charge transfer took place between TPP and the nanowire. In a separate experiment, we observed a clockwise hysteresis in the  $I_{DS}-V_{tip}$  curve when the tip was in contact with a TPP particle. In the case of an n-type semiconductor, the observed hysteresis direction suggested that the electron charging and discharging occurred from the nanowire side<sup>34)</sup>. The higher conductance of the AlGaAs barrier layer than that of the TPP particle also supported the charge transfer between TPP and the nanowire; the conductivities of the AlGaAs in the sample and TPP were  $21 \Omega^{-1}\text{cm}^{-1}$  and  $0.26 \Omega^{-1}\text{cm}^{-1}$ <sup>35)</sup>, respectively. The transport of electrons in the depleted AlGaAs barrier was probably caused by the electron having thermal energy that exceeded the potential barrier height. This is a major transport mechanism in the semiconductor Schottky barriers<sup>36)</sup>. In this mechanism, a thermally excited electron travels over the barrier within the mean free path. The sample used in this study satisfied this condition, where the electron mean free path in the AlGaAs was approximately 100 nm and was longer than the AlGaAs thickness of 60 nm. It is mentioned

that the analysis of the  $\Delta Z$  dependence of the RTS noise can systematically identify the charge exchange side. If the exchange of the electron occurs between the nanowire channel and TPP, the amplitude of the RTS will decrease by increasing  $\Delta Z$ , because  $C_1$  in Eq. (1) is decreased. On the other hand, the exchange occurs between the tip and TPP, and time constants of the RTS noise will be also increased by increasing  $\Delta Z$ , because the conductance between the tip and the molecule is exponentially decreased as a function of  $\Delta Z$ .

It is also necessary to confirm that the observed RTS noise was attributed to the TPP molecules, because there was also a possibility that the electron trap in the semiconductor surface caused the RTS noise<sup>13)</sup>. In this study, we considered the amplitude of the RTS noise. The RTS noise amplitude for the semiconductor trap in Ref. 13 was a few tens of nA order and it was larger than  $\Delta I_{DS}$  in this experiment shown in Fig. 3. This was because, in Ref. 13, the distance between the trap and the channel from the RTS amplitude was often smaller than the AlGaAs barrier thickness. This difference suggested that the observed RTS was probably attributed to the TPP molecules on the nanowire surface rather than the trap in the nanowire surface. However, further evidence is necessary for a clear confirmation of the TPP-related RTS noise. A possible approach is to examine the incident light wavelength selectivity of the RTS noise. If TPP contributes the observed RTS noise, the RTS should be sensitively changed by Soret-band light with a sufficiently high power. This is now under investigation.

Figure 5 shows histograms of the measured currents in the nanowire with TPP at  $V_{tip} = +3$  V shown in Figs. 3(c) and 3(e). Only a single peak appeared at  $V_{tip} = 0$  V as shown in Figs. 5(a) and 5(c). On the other hand, as shown in Figs. 5(b) and 5(d), multiple peaks appeared in the histogram at  $V_{tip} = +3$  V, which again indicated the charging and discharging of a discrete charge. Then, we decomposed the histograms at  $V_{tip} = +3$  V into multiple

Gaussian peaks. Both histograms could be fitted with two major peaks and two small peaks with the same peak intervals and the same deviations. The peak in the high current state corresponded to the electron emission of the TPP particle and that in the low current state corresponded to the electron capture of the TPP particle. The small peaks might arise from another charge state in the TPP particle. From the intervals between the major peaks, the RTS amplitude  $\Delta I_{DS}$  was evaluated to be 13 nA under both the dark and light conditions. On the other hand, the intensity balance of the two major peaks was different from each other. This suggested that the electron capture time constant  $\tau_c$  and the emission time constant  $\tau_e$  were modulated by the light, although the light did not excite TPP dealing with the observed RTS noise. The time constant ratios  $\tau_c/\tau_e$  evaluated from the decomposed peak intensities were 1.33 and 0.74 under the dark and light conditions, respectively. The increase in the emission time by the light irradiation indicated that the electron capture of the TPP particle was enhanced by the light. Considering the result of the increase in the DC current by the light irradiation as shown in Fig. 3, this was partly because the Fermi level of the nanowire channel was increased. This point is discussed later in this section.

Next, we examined whether the observed RTS noise arose from a single-electron charge event in terms of the RTS amplitude. A possible RTS amplitude was estimated from the equivalent circuit model as shown in Fig. 1(b) and it was compared with the experimental value. Using Eq. (1),  $\Delta I_{DS}$  caused by the channel potential change  $\Delta V$  is given by

$$\Delta I_{DS} = g_{m0} \Delta V = g_{m0} \frac{C_1 e}{C_1 C_2 + C_2 C_3 + C_3 C_1}, \quad (2)$$

where  $g_{m0}$  is the mutual conductance defined by the capacitance in the AlGaAs top barrier between the nanowire surface and the channel. For the quantitative evaluation of Eq. (2),  $C_1 = 4\pi\epsilon_0/[(\epsilon_{Air} d_{Air})^{-1} + (\epsilon_{TPP} d_{TPP})^{-1}]$  is used under the assumption that the tip and TPP are point

charges and the capacitance is given by the two point charges, where  $\epsilon_{\text{Air}}$  and  $\epsilon_{\text{TPP}}$  are the relative permittivities of air and TPP, and  $d_{\text{Air}}$  and  $d_{\text{TPP}}$  correspond to  $\Delta Z$  and the thickness of the TPP particle, respectively. Here the dielectric layer of  $C_1$  is considered to be formed by air and TPP with the thicknesses of  $d_{\text{Air}}$  and  $d_{\text{TPP}}$ , respectively. The electrostatically effective diameter of the molecule sphere is assumed to be 2 nm considering the molecular structure of TPP<sup>37)</sup> and the area where the electric field from the tip is concentrated on the nanowire top surface<sup>38,39)</sup>.  $C_2$  is estimated from the capacitance between the point charge on the nanowire top surface and the channel conductive plane, such as  $C_2 = 4\pi \epsilon_0 \epsilon_{\text{AlGaAs}} d_{\text{AlGaAs}}$ , where  $\epsilon_{\text{AlGaAs}}$  is the relative permittivity of AlGaAs, and  $d_{\text{AlGaAs}}$  is the AlGaAs top barrier thickness. Here the induced charge in the channel is distributed in the area with a width of  $2d_{\text{AlGaAs}}$ . The values of the relative permittivity of the AlGaAs and TPP are 12.2 and 4.6<sup>40)</sup>, respectively.  $C_3$  is negligibly small since the dielectric thickness was given by the substrate thicker than 350  $\mu\text{m}$ . We estimate  $g_{m0}$  from  $\nu_d C_2 W (2d_{\text{AlGaAs}} L)^{-1}$ , where  $L$  is the nanowire channel length,  $W$  is the channel width,  $\nu_d$  is the electron drift velocity in GaAs given by  $\mu V_{\text{DS}}/L$ , and  $\mu$  is the mobility of the channel carrier. In consideration of an elementary charge for  $e$  and its electrostatic effect reaching both channel sides, we obtained  $\Delta I_{\text{DS}}$  of 5.9 nA. This value reasonably explains  $\Delta I_{\text{DS}}$  of 13 nA from the decomposition of the current histograms in Figs. 5(b) and 5(d). The result of the analysis above indicates that our technique achieves a single-electron level charge sensitivity and the local enhancement of the charge sensitivity of the nanowire underneath the metal tip.

Finally, we discuss the tip bias dependence of the RTS noise. Figure 6 shows the energy level lineup of the TPP and GaAs system estimated from their material parameters. From Fig. 6(a), the relative energy difference between the lowest unoccupied molecular orbital (LUMO) of TPP and the conduction band edge  $E_C$  of the GaAs at  $V_{\text{tip}} = 0$  V is found to be

570 meV. This large energy difference results in the quite large time constant ratio, and the exchange of the electron between TPP and the GaAs nanowire is almost impossible. On the other hand, at  $V_{\text{tip}} = +3$  V, the energy level lineup is changed as shown in Fig. 6(b), in consideration of the bias dependence of each lineup estimated from the equivalent circuit model shown in Fig. 1(b). The energy difference between TPP and the GaAs is decreased by the tip bias and it is estimated to be 20 meV. On the other hand, assuming that the detailed balance is valid for the charging and discharging event, the ratio of the time constants is given by the next formula.

$$\frac{\tau_c}{\tau_e} = \exp\left(\frac{\Delta E}{kT}\right), \quad (3)$$

where  $\Delta E$  is the energy level difference between TPP and the GaAs channel,  $k$  is Boltzmann's constant, and  $T$  is temperature. The experimentally obtained time constant ratios of 1.33 and 0.74 at  $V_{\text{tip}} = +3$  V for the dark and light conditions gave  $\Delta E$  of 7 and -7 meV, respectively. These energies are reasonably in agreement with  $\Delta E = 20$  meV from the energy lineup. Therefore, in the experiment, the positive tip bias of +3 V aligned the energy levels of TPP and the GaAs channel, and promoted the frequent charge transfer between TPP and the GaAs channel, resulting in the RTS in the current. The change in  $\Delta E$  from 7 to -7 meV by the light irradiation might partly arise from the increase in the Fermi energy in the GaAs channel owing to the increase in the carrier density by the photoexcitation of many TPP molecules on overall the nanowire. From the change in the drain current of 0.2  $\mu\text{A}$  in Figs. 3(c) and 3(e), the change in the Fermi energy by the light irradiation was estimated to be 1 meV. This value was not far from 14 meV calculated using Eq. (3) with the experimentally obtained time constant ratios. From the discussion above, the obtained results are understood consistently if the observed RTS noise was attributed to the TPP charge dynamics. However,

there were still differences in the quantitative values. Further experiments and discussions are necessary for confirming that the observed charge dynamics arose from the TPP molecules and for the quantitative understanding of the overall behaviors.

## **6. Conclusions**

We investigated the detection of the charge dynamics of molecules using a GaAs-based nanowire where charge sensitivity was locally enhanced by molecule-metal tip capacitive coupling. The equivalent circuit model clarified that the capacitive coupling between the molecule and the metal tip enhanced the charge sensitivity of the nanowire at the tip contact position. A preliminary experimental investigation of the concept was made by using a GaAs-based nanowire with tetraphenylporphyrin (TPP) particles dispersed on the nanowire surface together with a measurement system integrating an atomic force microscope (AFM) and a dynamic current measurement monitor/spectrum analyzer. We could observe the RTS current noise when the tip was in contact with a TPP particle. Analysis of the RTS noise suggested that we observed the dynamic single-electron charge transfer between the TPP particle and the nanowire.

## **Acknowledgments**

The authors sincerely thank Professor S. W. Hwang of Korea University for valuable discussions. This work was partly supported by Grants-in-Aid for Scientific Research on Innovative Areas "Molecular Architectonics: Orchestration of Single Molecules for Novel Functions" (Grant Nos. 25110001 and 25110013).

## References

- 1) A. Aviram, *J. Am. Chem. Soc.* **110**, 5687 (1988).
- 2) J. Chen, M. A. Reed, A. M. Rawlett, and J. M. Tour, *Science* **286**, 1550 (1999).
- 3) R. L. McCreery and A. J. Bergren, *Adv. Mater.* **21**, 4303 (2009).
- 4) C. Jia, A. Migliore, N. Xin, A. Huang, J. Wang, Q. Yang, S. Wang, H. Chen, D. Wang, B. Feng, Z. Liu, G. Zhang, D. H. Qu, H. Tian, M. A. Ratner, H. Q. Hu, A. Nitzan, and X. Guo, *Science* **352**, 1443 (2016).
- 5) Z. J. Donhauser, B. A. Mantooth, K. F. Kelly, L. A. Bumm, J. D. Monnell, J. J. Stapleton, D. W. Price Jr., A. M. Rawlett, D. L. Allara<sup>1</sup>, J. M. Tour, and P. S. Weiss, *Science* **292**, 2303 (2001).
- 6) R. F. Service, *Science* **294**, 2442 (2001).
- 7) C. Xd, A. Primak, X. Zarate, J. Tomfohr, O. F. Sankey, A. L. Moore, D. Gust, G. Harris, and S. M. Lindsay, *Science* **294**, 571 (2001).
- 8) A. Terawaki, Y. Otsuka, H. Y. Lee, T. Matsumoto, H. Tanaka, and T. Kawai, *Appl. Phys. Lett.* **86**, 113901 (2005).
- 9) S. V. Aradhya and L. Venkataraman, *Nat. Nanotechnol.* **8**, 399 (2013).
- 10) A. van Houselt and H J. W. Zandvliet, *Rev. Mod. Phys.* **82**, 1593 (2010).
- 11) W. Steurer, S. Fatayer, L. Gross, and G. Meyer, *Nat. Commun.* **6**, 8353 (2015).
- 12) S. Inoue, R. Kuroda, X. Yin, M. Sato, and S. Kasai, *Jpn. J. Apple. Phys.* **54**, 04DN07 (2015).
- 13) M. Sato, X. Yin, R. Kuroda, and S. Kasai, *Jpn. J. Apple. Phys.* **55**, 02BD01 (2016).
- 14) P. Xie, Q. Xiong, Y. Fang, Q. Qing, and C. M. Lieber, *Nat. Nanotechnol.* **7**, 119 (2012).
- 15) G. Zheng, F. Patolsky, Y. Cui, W. U. Wang, and C. M. Lieber, *Nat. Biotechnol.* **23**, 1294

- (2005).
- 16) G. Zheng, X. P. A. Gao, and C. M. Lieber, *Nano Lett.* **10**, 3179 (2010).
  - 17) S. Mehrabani, A. J. Maker, and A. M. Armani, *Sensors* **5890**, 14 (2014).
  - 18) E. Baek, S. Pregl, M. Shaygan, L. Römhildt, W. M. Weber, T. Mikolajick, D. A. Ryndyk, L. Baraban, and G. Cuniberti, *Nano Res.* **1229**, 8 (2015).
  - 19) M. Yumoto, S. Kasai, and H. Hasegawa, *IOP Conf. Ser.* **184**, 213 (2005).
  - 20) T. Muramatsu, K. Miura, Y. Shiratori, Z. Yatabe, and S. Kasai, *Jpn. J. Appl. Phys.* **51**, 06FE18 (2012).
  - 21) K. Miura, Y. Shiratori, and S. Kasai, *Jpn. J. Appl. Phys.* **50**, 06GF18 (2011).
  - 22) M. A. Topinka, B. J. LeRoy, R. M. Westervelt, S. E. J. Shaw, R. Fleischmann, E. J. Heller, K. D. Maranowski, and A. C. Gossard, *Nature* **410**, 183 (2001).
  - 23) F. Martins, B. Hackens, M. G. Pala, T. Ouisse, H. Sellier, X. Wallart, S. Bollaert, A. Cappy, J. Chevrier, V. Bayot, and S. Huant, *Phys. Rev. Lett.* **99**, 136807 (2007).
  - 24) N. Aoki, R. Brunner, A. M. Burke, R. Akis, R. Meisels, D. K. Ferry, and Y. Ochiai, *Phys. Rev. Lett.* **108**, 136804 (2012).
  - 25) M. Lovcinský, J. Borecký, P. Kubát, and P. Jezek, *Gen. Physiol. Biophys.* **18**, 107 (1999).
  - 26) J. H. Woo, H. Yoon, J. H. Cha, D. Y. Jung, and S. S. Yoon, *J. Aerosol Sci.* **54**, 1 (2012).
  - 27) S. Urazhdin, W. K. Neils, S. H. Tessmer, N. O. Birge, and D. J. Van Harlingen, *Superconductor Sci. Technol.* **17**, 88 (2004).
  - 28) F. Hernández-Fernández, M. Pavanello, and L. Visscher, *Phys. Chem. Chem. Phys.* **18**, 21122 (2016).
  - 29) F. J. Williams, O. P. H. Vaughan, K. J. Knox, N. Bampos, and R. M. Lambert, *Chem. Commun.* **15**, 1688 (2004).
  - 30) A. M. Chizhik, R. Jäger, A. I. Chizhik, S. Bär, H. G. Mack, M. Sackrow, C. Stanciu, A.

- Lyubimtsev, M. Hanack, and A. J. Meixner, *Phys. Chem. Chem. Phys.* **3**, 1722 (2011).
- 31) F. N. Hooge, *IEEE Trans. Electron Devices* **41**, 1926 (1994).
- 32) L. K. J. Vandamme and F. N. Fooge, *IEEE Trans. Electron Devices* **55**, 3070 (2008).
- 33) M. J. Kirton and M. J. Uren, *Adv. Phys.* **38**, 367 (1989).
- 34) T. Nagumo, K. Takeuchi, T. Hase, and Y. Hayashi, *IEDM Tech. Dig.*, 2010, p. 628.
- 35) X. Zhai, D. Alexander, P. Derosa, and J. C. Garno, *Langmuir* **33**, 1132 (2017).
- 36) S. M. Sze, *Physics of Semiconductor Devices* (Wiley, New York, 1981) 2nd ed., p. 154.
- 37) V. C. Zoldan, R. Faccio, and A. A. Pasa, *Sci. Rep.* **5**, 8350 (2015).
- 38) T. Takahashi and S. Ono, *Ultramicroscopy* **100**, 287 (2004).
- 39) H. Hasegawa, N. Negoro, S. Kasai, Y. Ishikawa, and H. Fujikura, *J. Vac. Sci. Technol. B* **18**, 2100 (2000).
- 40) R. Jones and R.H. Tredgold, *Thin Solid Films* **99**, 25 (1983).

## Figure Captions

**Fig. 1.** (Color online) Concept of detection molecular charge dynamics utilizing metal tip-molecule capacitive coupling: (a) experimental setup and (b) schematic of the system with a layer structure of GaAs-based nanowire used as charge detector together with equivalent circuit.

**Fig. 2.** (Color online) (a) AFM image of fabricated GaAs-based nanowire with measurement circuit for characterization of field effect by the metal AFM tip. Tip positions for measurements are also indicated in the AFM image. (b) Example of measured current for various vertical tip positions, and average and root mean square of measured current as a function of (c) vertical tip position  $\Delta Z$  and (d) tip bias  $V_{\text{tip}}$ .

**Fig. 3.** (Color online) (a) AFM image of GaAs-based nanowire with TPP particles and measured currents: (b) tip on nanowire in dark, (c) tip on TPP in dark, (d) tip on nanowire under light, and (e) tip on TPP under light.

**Fig. 4.** (Color online) Measured low frequency noise spectra of nanowire currents in contact with TPP under dark condition at (a)  $V_{\text{tip}} = 0$  V and (b) +3 V, and under light condition at (c)  $V_{\text{tip}} = 0$  V and (d) +3 V.

**Fig. 5.** (Color online) Histograms of measured current in nanowire in contact with TPP under dark condition at (a)  $V_{\text{tip}} = 0$  V and (b) +3 V, and in light condition at (c)  $V_{\text{tip}} = 0$  V and (d)

+3 V.

**Fig. 6.** (Color online) Energy level diagrams of TPP, AlGaAs, and GaAs at (a)  $V_{\text{tip}} = 0$  and (b) +3 V.

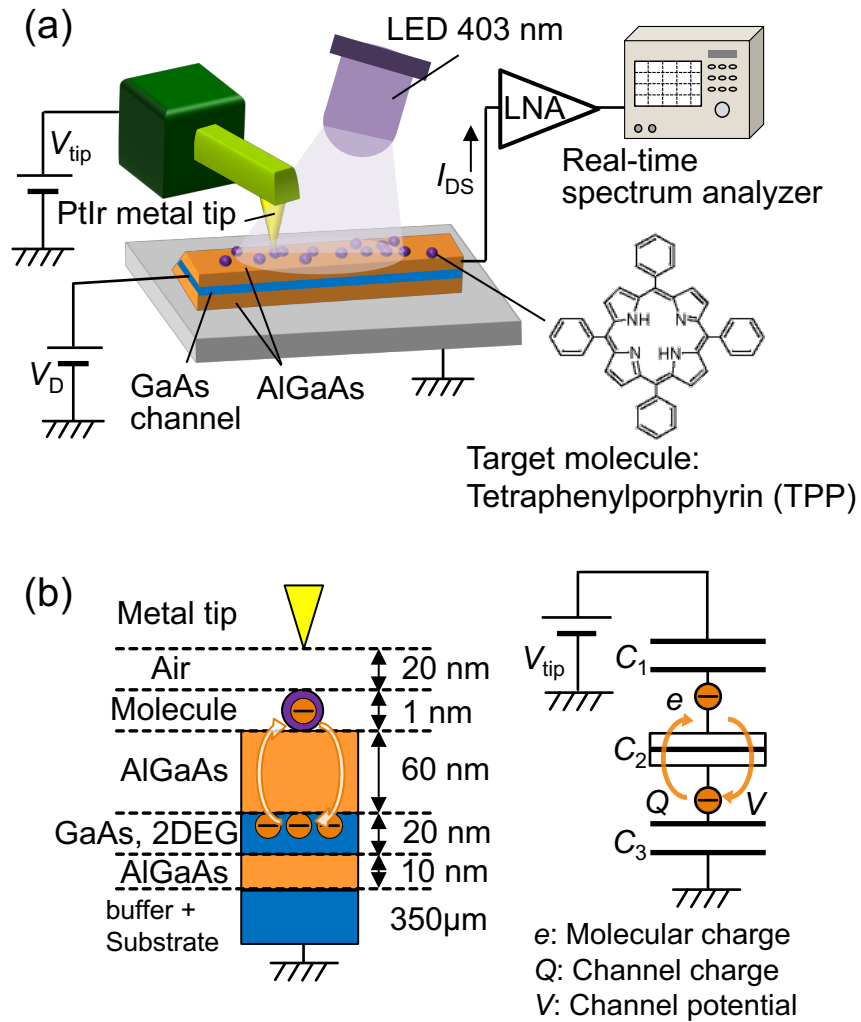


Fig. 1 Shoma Okamoto et al.

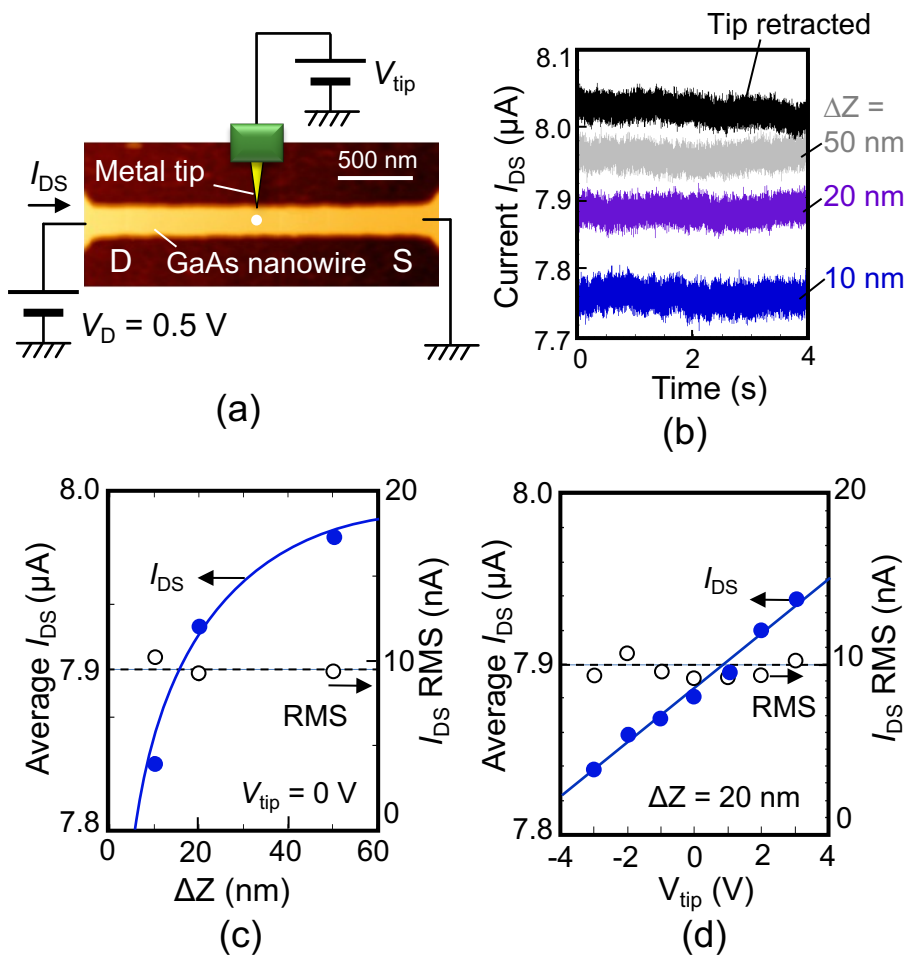


Fig. 2 Shoma Okamoto et al.

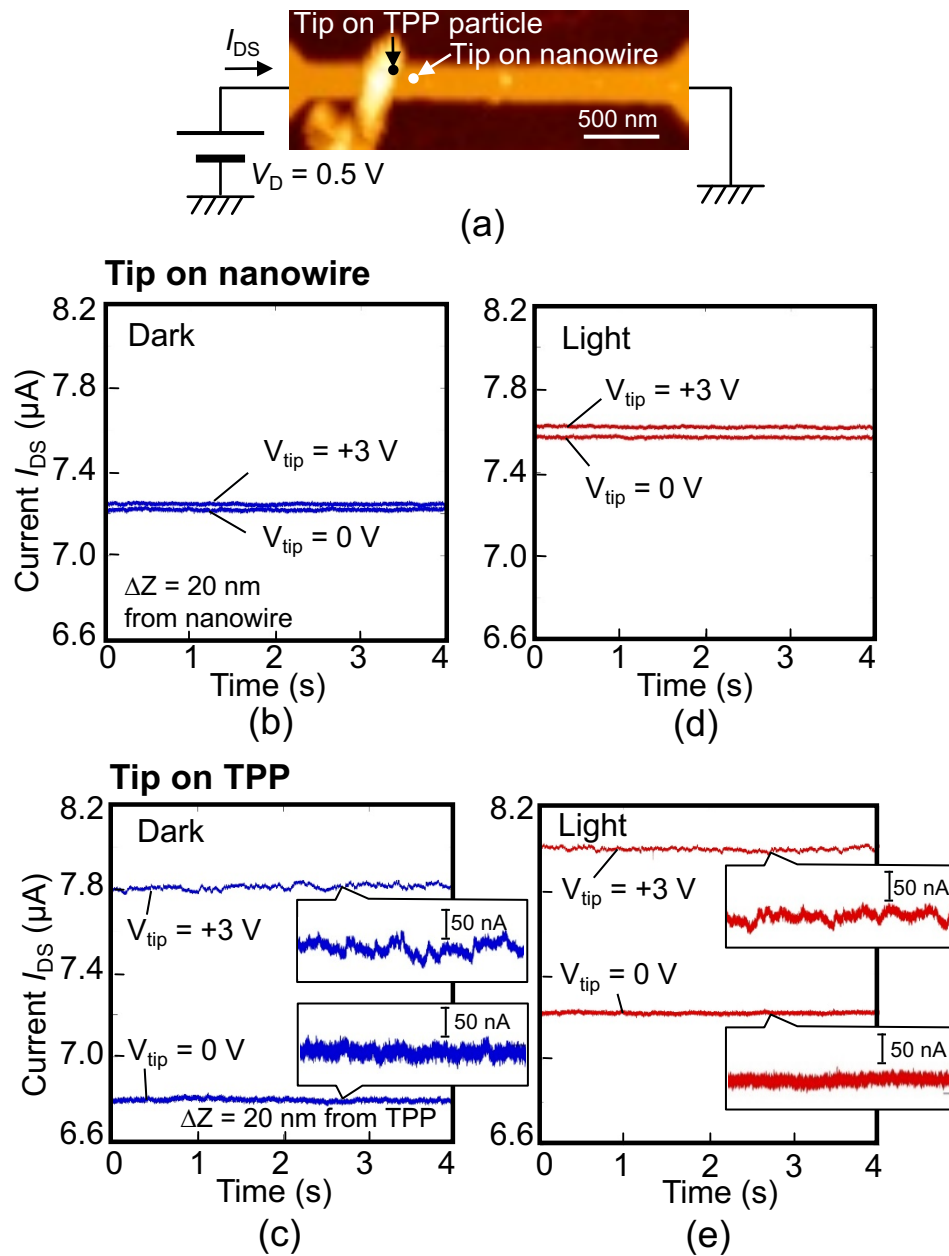


Fig. 3 Shoma Okamoto et al.

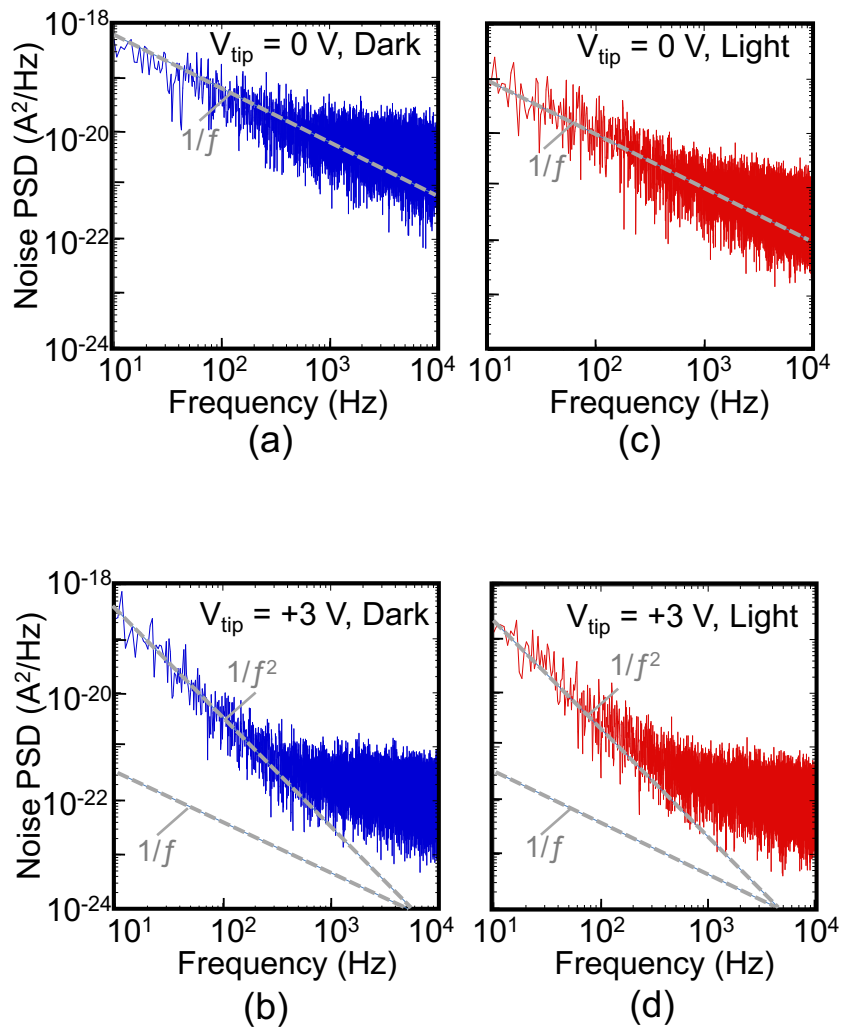


Fig. 4 Shoma Okamoto et al.

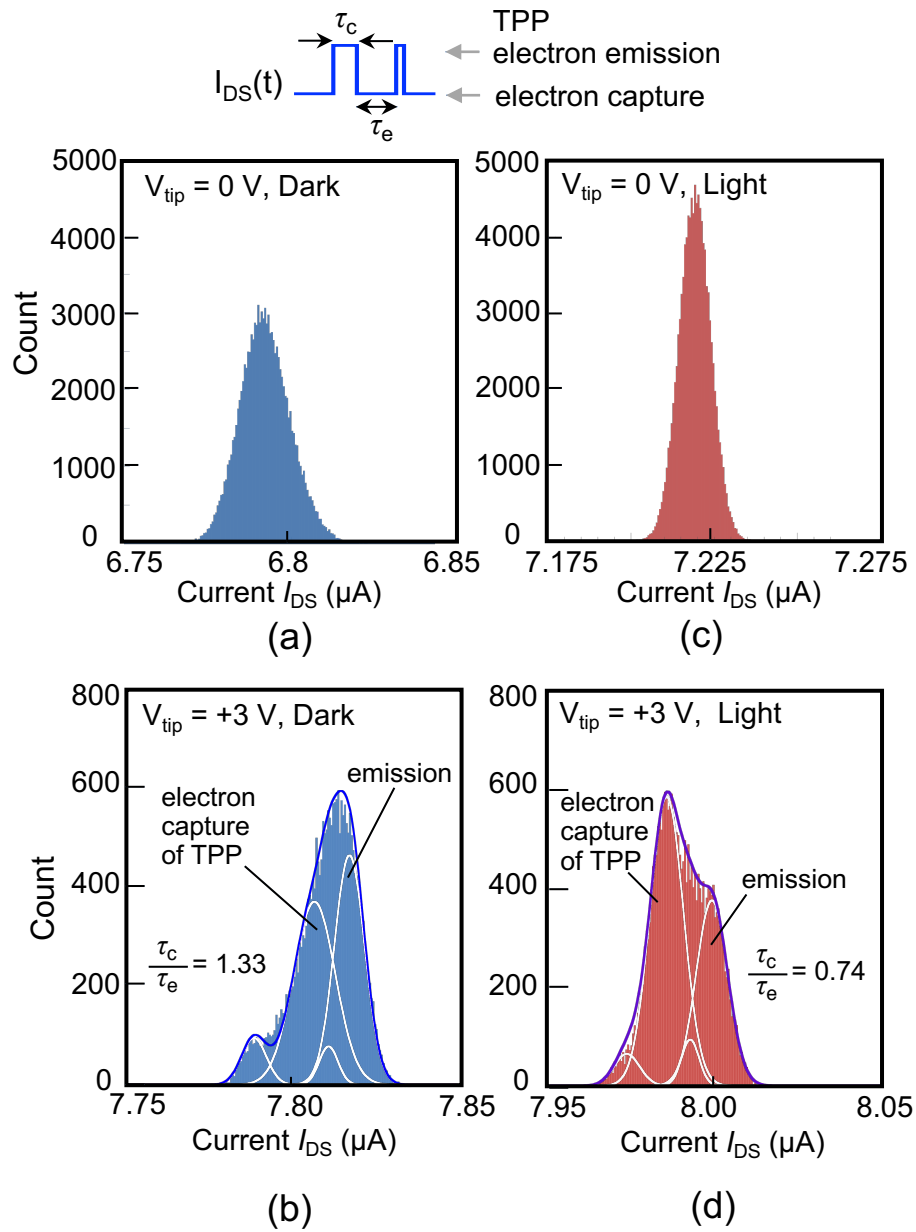


Fig. 5 Shoma Okamoto et al.

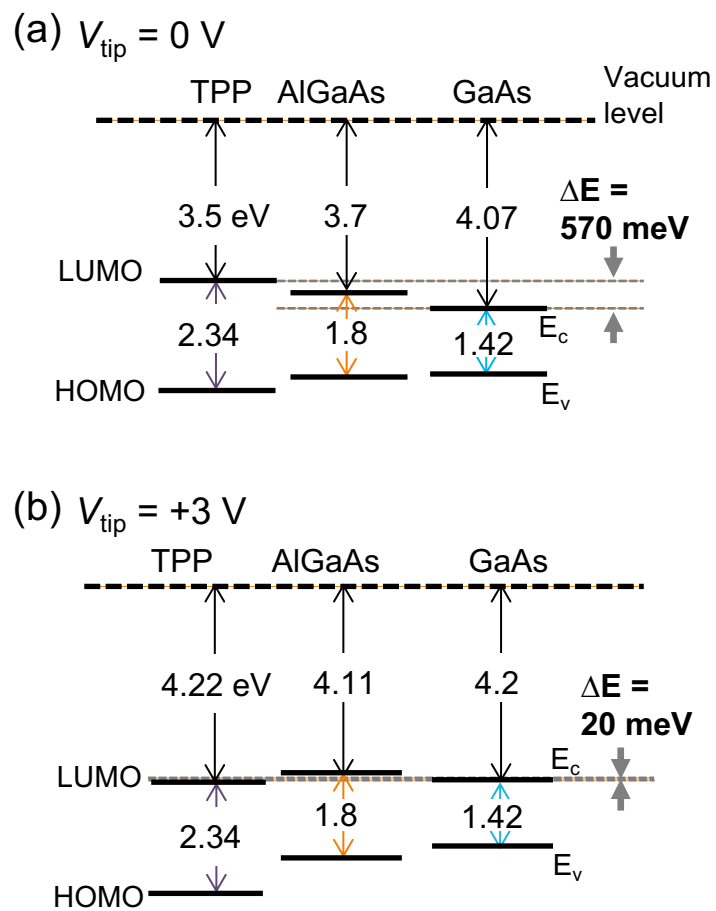


Fig. 6 Shoma Okamoto et al.